Chemical Engineering & Processing: Process Intensification 208 (2025) 110113

Contents lists available at ScienceDirect

Chemical Engineering and Processing - Process Intensification

journal homepage: www.elsevier.com/locate/cep

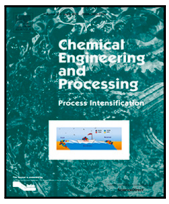

Additive manufactured helical micro distillation units for modular small-scale plants

Fabian Grinschek [a,*], Jannik Betz [a], Chen-Mei Chiu [a], Sören Dübal [a], Christoph Klahn [b], Roland Dittmeyer [a]

[a] Institute for Micro Process Engineering (IMVT), Karlsruhe Institute of Technology (KIT), Hermann-von-Helmholtz-Platz 1, Eggenstein-Leopoldshafen, Germany
[b] Institute of Mechanical Process Engineering and Mechanics, Karlsruhe Institute of Technology (KIT), Kaiserstraße 12, Karlsruhe, Germany

ARTICLE INFO

Keywords:
Additive manufacturing
Design for AM
Distillation packing
Micro distillation

ABSTRACT

The design and manufacture of microstructured distillation equipment is challenging. Additive manufacturing has the potential to facilitate the creation of new, efficient equipment. Our design of modular distillation units with helical flow path demonstrates this potential. We examined the separation efficiency at total reflux with cyclohexane/heptane. Due to the design being ready for manufacturing, various variants with different geometric parameters, including channel height and number of turns, were investigated. The experiments revealed that the primary helical structure is critical to separation performance and that unit coupling can enhance separation efficiency. Additionally, the impact of the mounting angle on separation performance was studied and verified. Especially at low loads, a significant increase was observed. Cold flow experiments using transparent 3D-printed resin columns demonstrate the influence of tilting on flow and aid in understanding the effect. Characterizations throughout the entire operating range, up to the flooding point, conclude the research.

1. Introduction

The energy transition to renewable energy sources increases the demand for modular, decentralized, small-scale (container-based) plants for the conversion at point of origin. Modular microstructured reactors are a viable approach, that is already commercialized [1]. Ideally, such plants also perform the refining and distillation of the products. Yet, this unit operation is challenging in such small-scale apparatuses [2,3]. First, enabling the counter-current flow and phase separation in smaller scales proves challenging due to the decreased influence of gravity compared to surface forces. Additionally, thermal management becomes demanding as heat losses and flow in walls significantly increase with downscaling. The literature only describes a relatively modest number of devices, mostly as initial prototypes. One principle frequently applied for small-scale units is known as horizontal distillation [4] or zero gravity distillation [5]. As the name suggests, the columns are oriented horizontal. On one end, the (micro) channel is heated to evaporate the liquid, while on the other end, the channel is cooled to condense the steam. The vapor flows from the hot end to the cold end, while the liquid flows in a counter-current direction, driven by capillary forces in a porous layer, using the heat pipe principle. The separation efficiency is high, but the throughput is relatively low, and heat management is challenging [6]. Tonkovich et al. achieved a height equivalent to a theoretical plate (HETP) of 13 mm in a micro slit oriented vertically [7]. Ziogas et al. proposed a different approach using a bubble column in a micro slit, achieving HETP values as low as 11 mm [8].

A further promising working principal between the vertical and the horizontal orientation is a helical flow path with low pitch as illustrated in Fig. 1. Combining the reduced effective gravity of the horizontal distillation with an enlarged flow path per height respectively length. Furthermore, secondary flows are induced by the centrifugal force, which could increase the mixing and help to reach higher separation performance. Already, early studies in the 1940s showed that the principal is promising, reaching HETP values between 10 mm to 20 mm with a low hold-up [9,10]. This involved winding a rectangular channel from a wire, which was wound around an inner tube in the form of a spiral, and then inserted into a glass tube. In the following years, a few designs based on this concept were proposed to reduce the prohibitive manufacturing efforts [11–14]. However, still these methods were demanding and needed, among others, etching or dissolving steps, so that with the advent of gas chromatography and spectroscopy as analytical methods the need for further development was reduced [15].

As additive manufacturing (AM) becomes more and more widespread, new possibilities are emerging in process engineering

* Corresponding author.
E-mail address: fabian.grinschek@alumni.kit.edu (F. Grinschek).

https://doi.org/10.1016/j.cep.2024.110113
Received 8 October 2024; Received in revised form 1 December 2024; Accepted 3 December 2024
Available online 10 December 2024

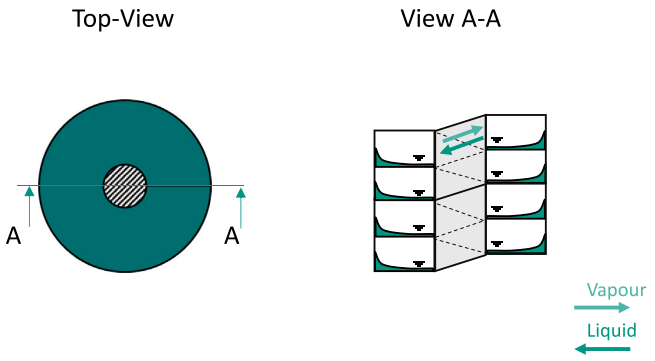

Fig. 1. Illustration of the basic working principle of the distillation apparatus with a helical channel. The boil up is flowing counter current to the liquid up the column. By the helical flow path, the length per height is increased and the effective gravity reduced. Thus, this results in a prolongation of the contact time.

also for such small-scale distillation units. Creating new avenues for the efficient manufacturing of complex shaped devices. For instance, Mardani et al. additively manufactured a complete modular distillation column [16]. Their helical design reached 4.6 theoretical stages with a hexane/cyclohexane mixture in an apparatus with a size of $112 \times 79 \times 151\,\mathrm{mm}^3$ ($w \times l \times h$). However, they faced resistance problems of the used polymers against the hydrocarbons distilled resulting in cracks and fouling. Neukäufer et al. recently developed additively manufactured packings for a lab scale distillation unit for the scale-up experiments [17]. Aiming for constant and reproducible separation efficiencies over a wide range of loads. Further research focuses on new (large scale) packing designs also coming up among others with helical designs for the flow path [18]. Additional, designs for packings with a helical liquid-bridge flow were proposed and subsequently validated through experiments [19,20]. In these apparatuses, capillary forces and gravitation direct the liquid to flow along a helically wound guide structure increasing the resident time [19,20].

In this work we explore the advantages of metal AM, namely powder bed fusion of metal using a laser based system (PBF-LB/M) [21] to overcome the described hurdles for the development and manufacturing of modular small-scale distillation units based on the helical flow principle. Two different types of "HeliDist" units are presented and tested: A single version (SV) for the principal investigations and a pluggable modular version (PV), which allows to couple different modules to increase the separation performance. By testing different types with different geometric parameters (number of turns, channel height) we identify the critical parameters. Moreover, an investigation is conducted into the angular dependency of the separation efficiency.

2. Design

The design process determines whether the advantages of AM can be exploited for a fast production cycle. A crucial step in this process is the immediate consideration of design guidelines to shorten the post-processing and printing steps [22]. In particular, post-processing can significantly prolong the evaluation process of different designs. The following section presents therefore the fundamental design considerations of the HeliDist units.

The basic working principal, shown in Fig. 1, is not feasible to manufacture by the PBF-LB\M process due to the requirement for support structures for overhanging features at angles below 45° relative to the horizontal [23]. The helical channel in vertical orientation would result in such overhanging walls and need supports structures in the channel. The removal of such structures in winding channels would be very time consuming, if not impossible. To circumvent this we adapted the design to this manufacturing-related restriction [24] by tilting the central axis of the helix by 45°. Therefore, however, the apparatus must be mounted in a 45° angle in operation as shown in Fig. 2. We have also to mention, that by keeping the cylindrical outer shape the channel top and bottom surface is no longer an annulus but is elliptical. Since we assume a better mixing of the flow through the widening and narrowing of the channel, we kept the elliptical shape of the center line. For instance, sinusoidal channels were already proposed for the application in micro distillation apparatuses [25] and showed an increase in heat transfer for helical channels [26]. Owing to the fact that typical PBF-LB/M systems have production rates only in the range of a few $\mathrm{cm}^3\,\mathrm{h}^{-1}$, thin walls are preferred to minimize printing time. Increasing thereby, furthermore, the utilized volume and simultaneously reducing the thermal heat conduction through the apparatus. Therefore, we developed a strategy to print leak-free thin walls with around 250 µm wall tickness as we already published [27]. The diameter of the cylindrical outer and inner wall was set to 25 mm respectively 5 mm. To ensure phase separation in the top and the bottom of the units the distance between the top and the bottom wall to the spiral turns was increased to $h_{top/bottom} = 2 \cdot h_{channel}$. Following this basic design considerations for the core of the units, two connecting designs were developed: a single unit design (Figs. 2 and 3) and a pluggable version (Figs. 5 and 6). For the first principal investigation, all connectors were positioned on the base, thereby reducing the overall height of the unit. Since the apparatus is fixed to the build platform after printing and must be removed by sawing after printing, all post-processing steps can subsequently carried out in one plane in the single design. Pre-printed M5 threads were chosen for the connections of the apparatus, onto which pneumatic screw-in plug-in fittings are mounted. They are compact and moreover allow a quick assembly and disassembly. Besides, there are male and female connectors available to couple different units. On the base a surrounding 20 mm high wall is printed for the clamping in a machine vice (see also Fig. 4). To reduce heat loss by conduction into this frame, it was positioned as far away as possible from the actual structure. At the same time, it was also necessary to utilize the build space. The outer dimensions were therefore chosen so that four apparatuses can be printed on one build plate of the used PBF-LB/M-system. If the units should be coupled the single version would require an additional pump to feed the liquid in the next unit. Therefore the pluggable version was designed, with two connectors on top, which allows to stake the units as shown in Fig. 6(b). In the pluggable version the frame is extended hollow to support the connectors at the top. This allows an easier isolation of the units by filling the space with glass fiber mats (see also Fig. 6(a)). The parametric CAD design was created in Autodesk Inventor© (United States) with all parameters stored in an Excel© file. Modifying the parameters of a unit, such as the height of channels or the number of turns, requires only the time to verify that all changes have been correctly implemented.

3. Manufacturing and characterization

3.1. Manufacturing

This study used a Realizer 125 PBF-LB/M system (DMG Mori, Germany), equipped with a 400 W yttrium fiber laser and a build volume of $125 \times 125 \times 200\,\mathrm{mm}^3$. The parts were produced by fusing stainless steel 316L powder with a particle size of 10–45 µm (Carpenter Additive, UK). After depowdering the units were removed from the build plate and the bottom surface was face-milled. After recutting the threads a leak test was conducted. If minor leaks were detected, they were closed with chemical and temperature resistant resin. After isolation with glass fiber mats the units where ready to use.

3.2. Test rig

The aim of the test rig is to experimentally characterize different units with regard to its separation efficiency. Thereby, an important consideration was also to allow a quick change between different units.

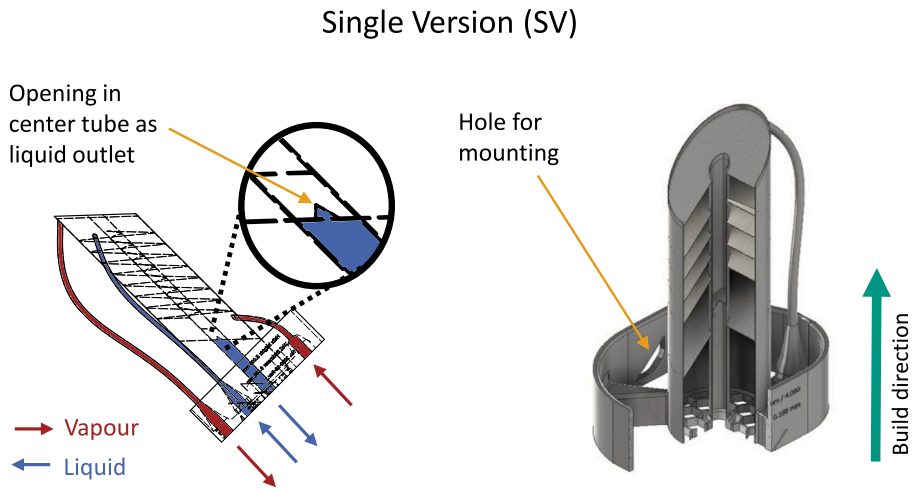

Fig. 2. Drawing of the single versions of a HeliDist unit with 8 turns (left) and 3D-representation of a three-quarter cut of a HeliDist unit with 4 turns (right). The drawing left shows the unit at an installation angle of 45°. The single version has all M5 connection threads at the base, which reduces post-processing and printing time. The central tube thereby also serves as a connection tube for the bottom liquid flow (detail view).

Fig. 3. Picture of a manufactured single version HeliDist unit with 10 turns and a channel height of 5 mm.

The test rig follows a plant concept for micro distillation apparatuses by Sundberg et al. [28] that operates distillation apparatuses with defined flow rates. Fig. 7 shows the flow diagram of the test system. To mount the HeliDist units, an M4 screw approximately 5 cm long was inserted through a hole in the frame (see also Fig. 2 right) and secured with a nut. This screw was then used to fasten the unit onto an aluminum strut profile. The distance of approximately 3 cm ensured minimal heat conduction. The HeliDist units were fixed at a 45° angle to the horizontal plane. The complete apparatus was then insulated with glass fiber mats. The procedure was the same for coupled units. The units were then connected via flexible insulated PTFE-tubes so that apparatuses with different inclination and connection positions can be connected. A micro annular gear pump (HNP Microsystems, Germany) feeds the outgoing liquid from the bottom of the units into a microstructured crossflow evaporator. This evaporator features 35 microchannels (0.5 mm × 0.5 mm × 60 mm) on the evaporating side. Thereby, the liquid hold-up is low, with the total volume of the channels, including the inlets and outlets, being below 5 mL. The temperature of the heating oil of the evaporator was set so that the vapor exits at least 10 K superheated. By heat traced hoses and tubes it was ensured that the vapor did not condense in them.

Compared to the setup of Sundberg et al. a dedicated cooler of the condensate in front of the pump was omitted. The dissipated heat flux in the not insulated tubes in front of the pump was high enough to cool down the stream. Coriolis flow sensors (Bronkhorst, United States) were used to measure the density and mass flow of the bottom flow. The liquid level in the bottom was quantified by hydrostatic pressure with a differential pressure sensor. The transparency of the PTFE tubing allowed the level to be visually checked by briefly removing the insulation and setting the set-value for the pressure controller. The level was controlled by the output of the pump for the condensate from the condenser. The vapor was condensed in a lab scale spiral cooler made of glass (Lenz-Laborglas GmbH, Germany, area 240 cm^2, length 160 mm), which was tempered by chilled water from a thermostat (Julabo, Germany). Downstream of the spiral cooler is a small collecting vessel, which allows the system to be filled. The pressure was equalized to the environment via a capillary. This condensate flow was pumped by a micro annular gear pump into a microstructured heat exchanger where the flow could be preheated. All temperatures where measured by PT-100 probes (Conatex, Germany). The lab scale plant was controlled by a laboratory control system (Hitec-Zang, Germany).

3.2.1. Distillation tests

For the separation efficiency tests an equimolar mixture of cyclohexane and heptane was used. After the heat up, the bottom pump was set to a defined mass flow and the liquid level in the bottom of the column was controlled to a level just below the connector with the condensate flow. When the liquid levels and the density of the top and bottom remained constant for at least 30 minutes, a 1 mL sample was taken from each of the top and bottom streams using a syringe. The taken volume was replaced accordingly by fresh mixture. The samples were then analyzed by gas chromatography (Agilent G1530A, USA). The repeatability was good, with a deviation of less than 0.1 theoretical plates between repeated measurements under consistent operating conditions and mounting positions. However, the influence of the mounting angle deviations should be noted here and will be discussed further in the following sections.

3.2.2. Heat loss measurement

To determine the heat losses, distillation experiments were carried out at total reflux with the pure cyclohexane and heptane similar to Mardani et al. [16] and Sundberg et al. [28]. This ensured a constant

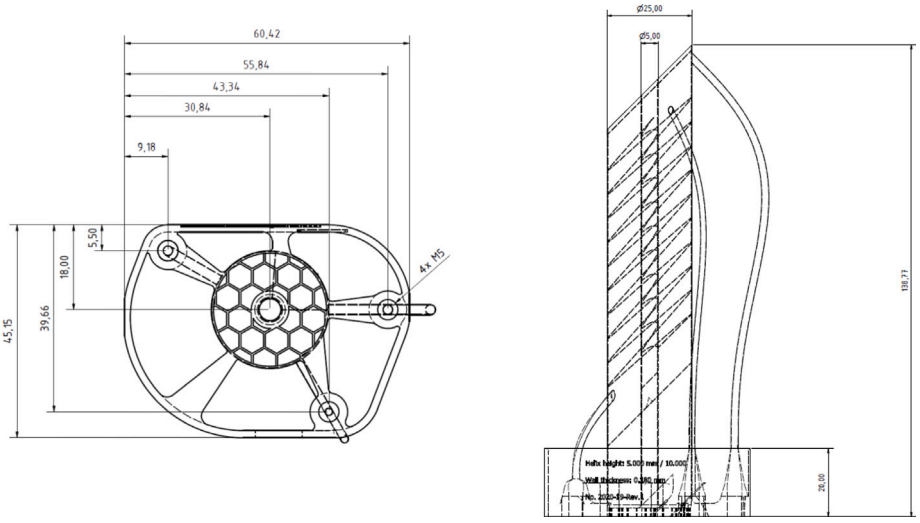

Fig. 4. Dimensioning of a single-version HeliDist unit with 10 turns and a channel height of 5 mm. Left: Bottom view. Right: Side view.

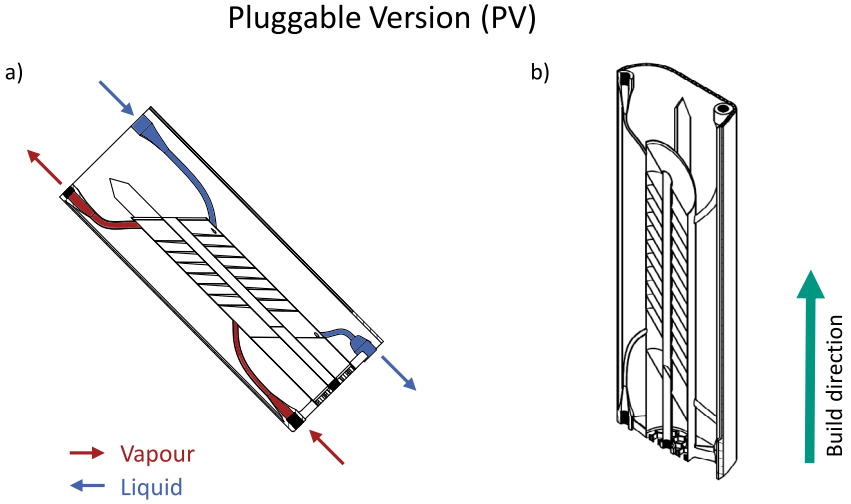

Fig. 5. Drawings of pluggable versions of a HeliDist Unit. (a) Cross-cut through a apparatus with 8 turns in the operation position of 45°. The connection pipes for the steam are highlighted in red and for the liquid in blue. (b) 3D-representation of the cross cut showing also the build direction of the additive manufacturing system.

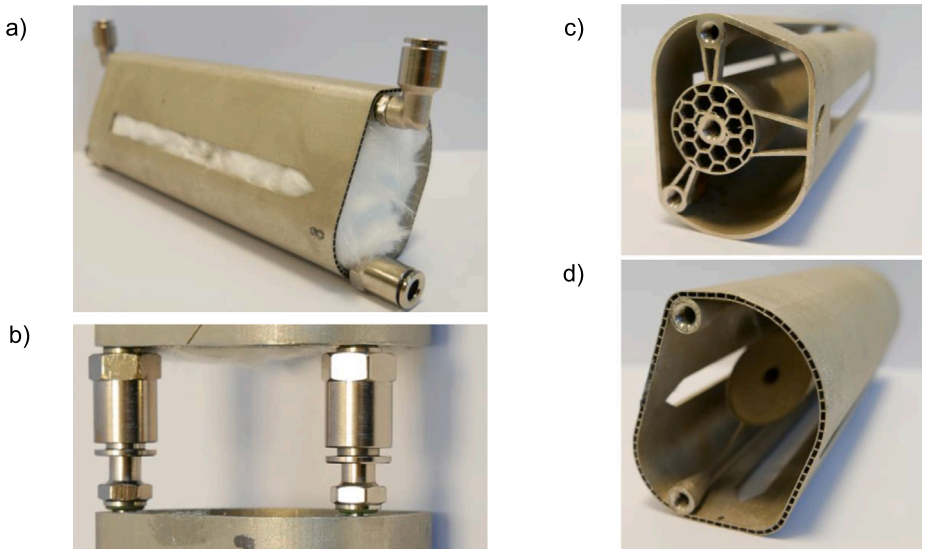

Fig. 6. Close-up pictures of the PV version: (a) Unit filled with glass fiber mats as isolation and mounted pneumatic fittings (b) Close-up of the coupling between two units with male and female pneumatic fittings. (c) Bottom view without fittings. (d) Top view without fittings.

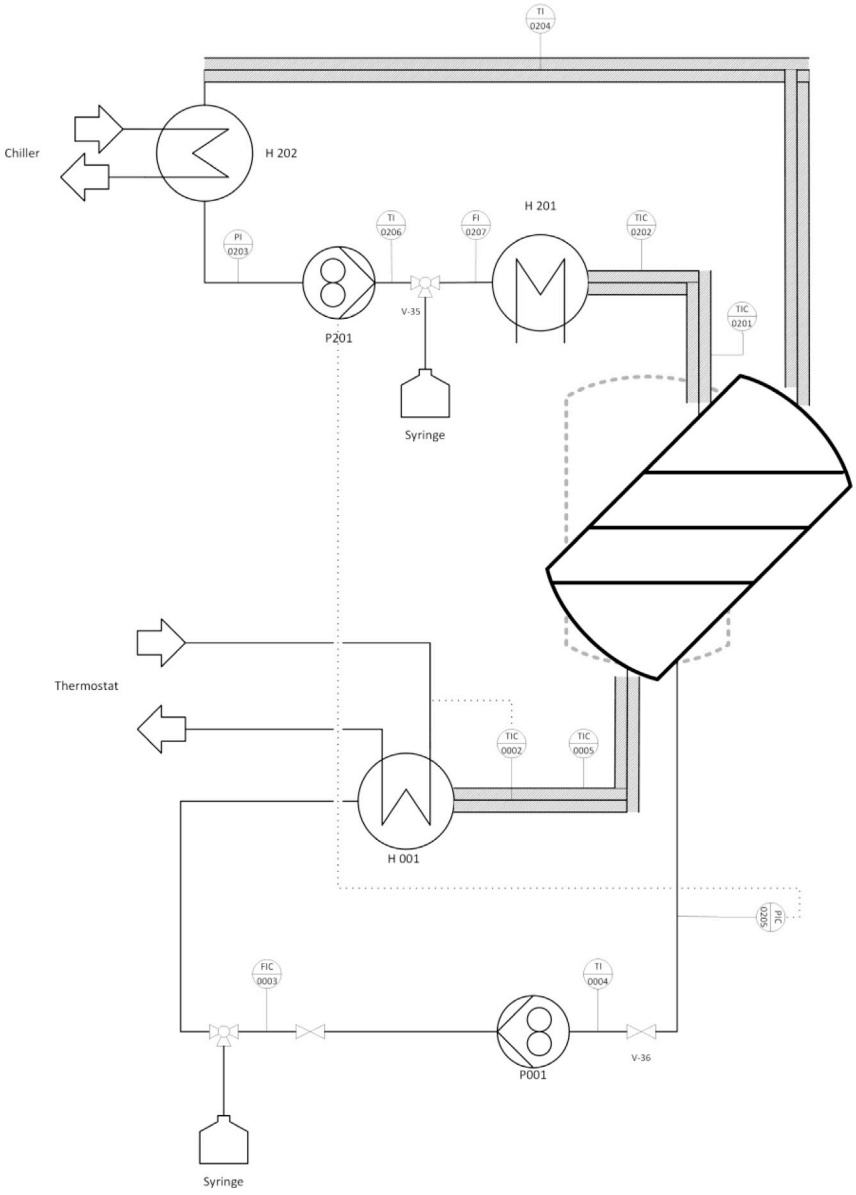

Fig. 7. Piping and instrumentation diagram of the test rig. The columns could be mounted with variable inclinations.

defined temperature (boiling temperature of the pure substances) inside the apparatus. The heat losses can then be calculated from the energy balance according to Eq. (1) (see also [16,28]) using the measured mass flows $\dot{m}_{\mathrm{bottom}}$ and $\dot{m}_{\mathrm{bottom}}$. Further with the measured temperatures of the inlet and outlet streams and the data from [29] the specific enthalpies h can be calculated.

$$\Delta Q = \dot{m}_{\mathrm{bottom}} \cdot \left(h_{\mathrm{vapour,in}} - h_{\mathrm{liquid,out}}\right) - \dot{m}_{\mathrm{top}} \cdot \left(h_{\mathrm{liquid,in}} - h_{\mathrm{vapour,out}}\right) \quad (1)$$

3.2.3. Angular dependency

An optimized fixture for the HeliDist units was used to study the effect of angular misalignment on separation efficiency. With the standard fixture using only a screw, the mounting angle could change slightly during the installation step. The optimized fixture is shown in Fig. 8. The angular position is fixed by tongue and groove joint fitting using the parallel surfaces of the hole depicted in Fig. 2 of the HeliDist units. The base plate of the fixture was then fixed to the frame of the test stand. Thereby the inclination of the units could be measured and adjusted with a digital level protractor (Voltcraft, Germany) also in operation without the need to remove the isolation. This minimizes the risk of changing the orientation in this step.

3.2.4. Hold-up measurements

To further investigate the influence of angular deviations, hold-up measurements were also examined at different mounting angles. The experiments followed a similar approach to that used in the distillation experiments. The main difference was that pure cyclohexane was used to avoid a change in density due to different compositions. At a constant boiler mass flow of $150\,\mathrm{g\,h^{-1}}$ and after reaching constant liquid levels the angle was changed. Then the bottom level was set to the same liquid level, thereby increasing respectively decreasing the liquid level after the condenser. This amount was taken respectively refilled then with a weighted syringe. To compensate for small leak flows, the base point was approached between the measurements and thereby the mass balance was closed.

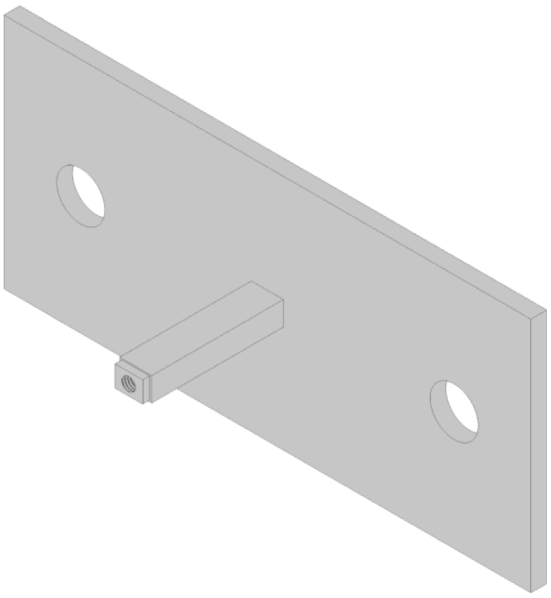

Fig. 8. Optimized fixture for the apparatuses. The angular position is fixed by tongue and groove joint fitting using the parallel surfaces of the hole depicted in Fig. 2 of the HeliDist units.

Table 1
Results of the heat loss experiments with a HeliDist unit with 9 turns and a channel height of 5 mm.
Source: Data for the boiling point from [29].

Chemical	Boiling point [°C]	$\dot{m}_{bottom}$ [g h^{-1}]	$\dot{m}_{top}$ [g h^{-1}]	ΔQ [W]
Cyclohexane	81	157	101	5.3
Heptane	98	149	58	7.0

3.3. Qualitative cold flow visualization

The countercurrent flow in the apparatus is qualitatively evaluated in additively manufactured transparent units. The parts are produced by vat photopolymerization on a Formlabs 3BL (United States) machine. The units have a channel height of 5 mm and a wall thickness of 1 mm. A syringe pump fed inked cyclohexane into the unit and a mass flow controller (Bronkhorst, United States) dosed an Argon gas stream to mimic the corresponding volume flow of evaporated cyclohexane. The liquid level in the bottom was controlled by the corresponding pipe principal described in [16,30] to prevent a bypass gas flow through the liquid outlet. The installation angle was adjusted with the digital protractor directly on the units.

4. Results and discussion

4.1. Heat losses

In Table 1, the results for heat loss measurements of a HeliDist unit with a modular design and 9 turns are shown. As expected, heat losses increase with rising temperature. Compared to literature values, the measured heat losses are lower. For example, Mardani et al. [16] reported heat losses around 9.9 W for their apparatus with a cyclohexane mass flow rate between 110 g h^{-1} to 120 g h^{-1}, whereas the measured heat losses for the HeliDist unit are only 5.2 W. Sundberg et al. also reported higher heat losses for their apparatus [28]. However, for a complete adiabatic operation, further investigation into (active) insulation concepts will be necessary in future studies.

Table 2
Results of the first screening test with SV-units with 4 turns and different $h_{channel}$ at total reflux.

$h_{channel}$ [mm]	$\dot{m}_{bottom}$ [g h^{-1}]	n_{theo} [–]	$HETP_{Helix}$ [mm]
≤ 4	Flooded	–	–
5	150	1.2	17
6	142	0.8	30
7	151	0.9	32
8	145	1.1	34

4.2. Influence of channel height

The initial series of experiments was designed to identify the optimal geometric dimensions of the helical channel. These screening tests examined 7 units with 4 turns and varying channel heights $h_{channel}$ of 2 mm to 8 mm. Single version units with $h_{channel} < 5$ mm did not reach a stable operating point without flooding. We identified the flooding of a unit, when the flow in the top of the column could be significantly greater than the steam flow of the boiler without changing the bottom liquid level. Between $h_{channel} = 5$ mm to 8 mm the separation efficiency was for all units in the same range of $n_{theo} \approx 1.0$ theoretical plates as shown in Table 2. Obviously, the *HETP*-value was the lowest for 5 mm so it was decided to fix $h_{channel}$ to 5 mm for the further investigations.

4.3. Influence of number of turns

The relatively low number of approximately 1.0 theoretical plates for the HeliDist Units with 4 turns does not allow the measured separation efficiency to be attributed specifically to the "core design"—the helical channel—or to the inlets and outlets. The parametric design and the short printing times allows to easily change the number of turns and actually measure the separation efficiency for various n_{turns}. Through this, influences of the in-, outlets or the test rig itself could be separated and an actual $HETP_{Helix}$ value could be derived of the ratio between the slope of n_{theo} and n_{turns} according to Eq. (2)

$$HETP_{Helix} = \frac{\Delta n_{turns}}{\Delta n_{theo}} \cdot h_{Channel} \quad (2)$$

Fig. 9 shows the results of this tests with different units with 2 to 16 turns for a load of $m_{bottom} = 150$ g h^{-1}. The results of the single

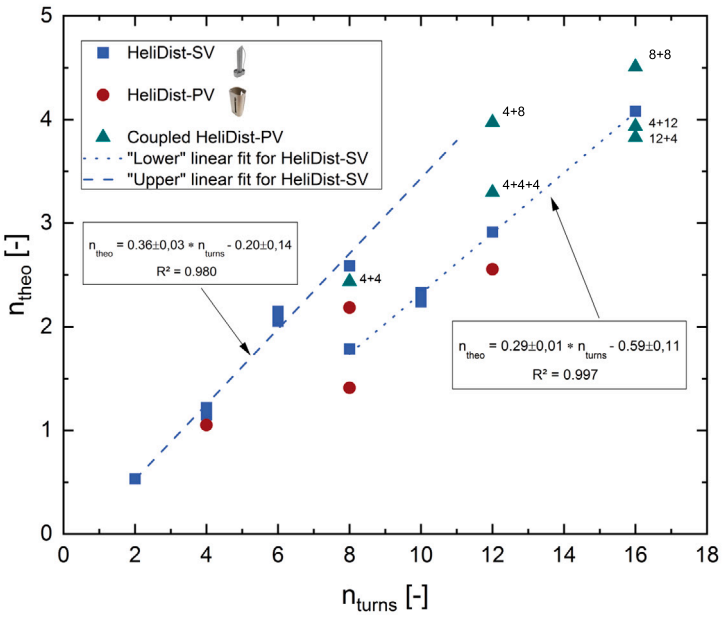

Fig. 9. Results of the separation performance tests dependend on the number of turns for the different types of HeliDist units. For the SV with $n_{turns} \geq 8$ respectively $n_{turns} \leq 8$ a linear fit is indicated. Coupled PV-units are indicated by "X+Y", where X is indicating the number of turns n_{turns} of the lower unit and "Y" of the top unit respectively.

modules show that there is a correlation between the number of turns and the separation efficiency. The measurements also reveal that there are at least two stable operating states. For example, the single unit with 8 turns showed two stable states with a lower value of $n_{theo} = 1.8$ and higher value $n_{theo} = 2.7$. It seemed that the number of turns is a critical factor, if the separation factor is in the upper or lower value band. As for the single units with $n_{turns} \geq 8$ a linear correlation with a $HETP_{\mathrm{Helix}}$-value of around 17 mm was found. Whereas for $n_{turns} \leq 8$ a $HETP_{\mathrm{Helix}}$-value of around 14 mm was reached showing the upper range. Measurements with non-coupled PV units showed a similar behavior, with values slightly below the SV units. Moreover, up to 3 coupled units could also be successfully operated and is showing that the coupling is possible to scale-up the number of theoretical plates.

Podbilinak et al. described a similar effect of two states and allocated them to a pre-flooded or dry starting condition [9]. However, as compared to their studies the HeliDist units are designed with a relatively low number of n_{turns}, so a complete flooding happens fast in the start-up of the units and a "dry" start is challenging. A detailed look into the liquid level data of the experiments revealed, that pre-flooded units showed also results in the lower range. Further, Podbielniak fitted the porous body into a glass tubes, thereby flooding could have prevented a by-pass flow in a gap between the helical packing and the glass tube. This could be excluded due to the manufacturing in one piece. So these results do not confirm an influence of the starting conditions on the separation efficiency.

4.4. Influence of angular deviations of the mounting position on the separation efficiency

The helical channels have a relatively low incline in relation to the horizontal plane. Therefore, even a minor deviation in the mounting angle during installation could impact the separation efficiency. To investigate the influence of the operating angle, a more rigid and adjustable fixture for the modules was utilized. The angle was varied for modular units with 4, 8, and 12 turns at a constant load of $m_{bottom} = 150\,\mathrm{g\,h^{-1}}$. The separation efficiency was determined and is illustrated

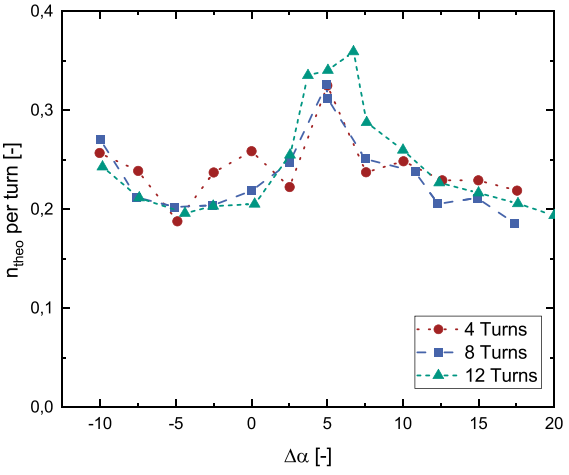

Fig. 10. Separation efficiency n_{theo} per turn versus the angular deviation $\Delta\alpha$ for PV-units with $n_{\mathrm{turns}} = 4$, 8 and 12 at $\dot{m}_{\mathrm{bottom}} = 150\,\mathrm{g\,h^{-1}}$.

in Fig. 10. The influence of the installation angle was not symmetrical, both in terms of the shape of the angle dependency of the separation performance as in the angular operation range. Counterclockwise the units could be tilted between −7.5° to 0° and the separation efficiency was quite stable and only for high deviation of $\Delta\alpha = -10°$ an increase was observed close to the operation limit. Whereas clockwise there is a small range around 5° where the separation efficiency is roughly two-times higher than around the nominal angle $\Delta\alpha = 0°$. These observations are in agreement with the results from Section 4.3, were especially the results in the lower separation range showed a clear linear relationship with the number of turns. A symmetrical influence around the nominal angle would have led to more scattered results. The units fixture was in the frame in the lower part, so tilting in negative direction is more likely as the HeliDist units gets larger, as the tubes

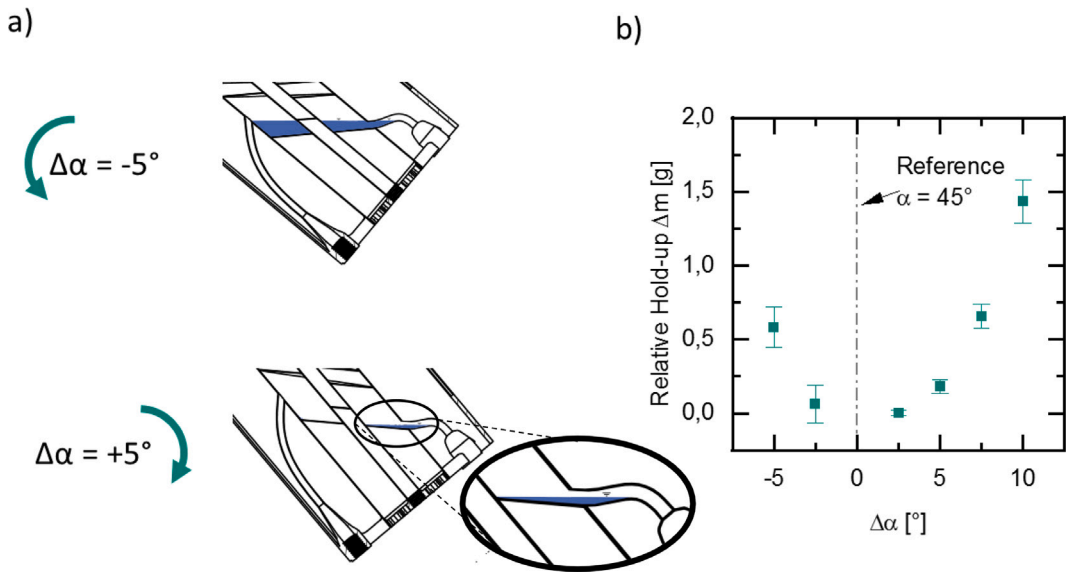

Fig. 11. Effects of tilting on the liquid hold-up of the column. (a) Liquid level in the bottom of the column for a tilt of 5° counter- and clockwise. When the units are tilted counter clockwise the liquid level is increased due to the higher position of the outlet. (b) Results of the hold-up measurements depending on the angular deviation $\Delta\alpha$ for PV unit with $n_{\text{turns}} = 12$.

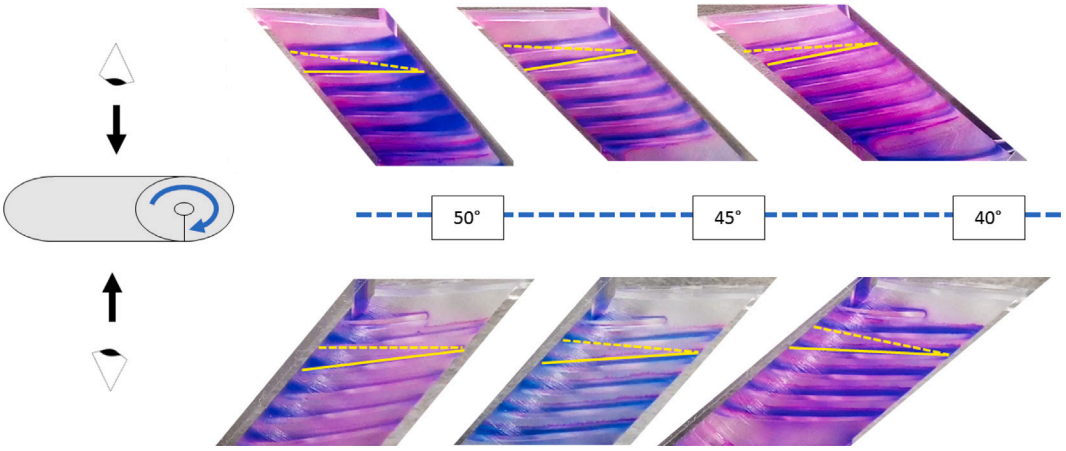

Fig. 12. Cold flow visualization with transparent units and blue colored cyclohexane with a $\dot{m}_{\text{cyclohexan}} = 150\,\text{g}\,\text{h}^{-1}$. Pictures show units with different inclination of $\alpha = 40°$, 45° and 50°. Yellow lines are indicating the slope of the outer path on the helix of the channel. The solid lines represent the front line in the viewing direction and the dashed line the back line (see also Eq. (3)).

and the apparatus' own weight exerts a greater torque in this direction. This explains, why the units with $n_{turns} \geq 8$ showed lower separation efficiencies and also the coupled units showed a higher scattering. The difference in the angular operations limits could be explained by the fact, that the minimum liquid level of the outlet is depending on the angle as shown in Fig. 11(a). With a counterclockwise turn the liquid level at the bottom increases since the vertical position of outlet rises and a siphon is created. Thereby, increasing the chance for a liquid entrainment. In clockwise direction this is not the case. Fig. 11(b) depicts the dynamic hold-up of cyclohexane depending on the angle for a unit with 12 turns. While at 5° the hold-up is only increased by approximately 0.2 g, whereas at −5° it is already increased by 0.6 g. It is therefore reasonable to assume that an effect at the inlet or outlet could also be a possible explanation for the differences in the separation performance. However, the results of the distillation experiments show that this is not the case, since the number of theoretical plates per turn stay about the same regardless whether a unit with 4, 8 or 12 turns is used. Therefore the decisive effects must influence the flow in every turn.

Cold flow measurements with inked cyclohexane in transparent columns visualized the flow (Fig. 12). A tilt in positive direction raises the level of the liquid up to the top of the channel, whereas this is not the case in the other direction. This increases the wetted surface area and facilitates the remixing of the liquid flow. Both effects could increase the separation performance. The effect can be explained by the asymmetry in the channel cross-section. On one half of the channel, the inner tube forms an acute angle and the outer tube forms an obtuse angle, while the opposite is true on the other half (also see Fig. 2). Thereby, with a turn in this direction of the acute angle the liquid is pent up due to the narrowing of the cross section due to the acute angle. Furthermore, it has to mentioned, that tilting the units increases the pitch of channels on one half of a turn, whereas it is decreased on the other half. Following basic geometric considerations a simplified equation for the average slope (as shown with the yellow lines in Fig. 12) in z-Direction (Gravitation) is proposed in Eq. (3):

$$\alpha_{\text{channel}} \simeq \pm \arcsin \frac{0.5 \cdot h_{\text{channel}}}{\sqrt{2} \cdot d_{\text{channel}}} \approx 4.1° \tag{3}$$

Which is in good agreement with the maximum separation efficiency n_{theo} at an angular deviation $\Delta\alpha \approx \alpha_{\text{channel}}$ as seen in the distillation

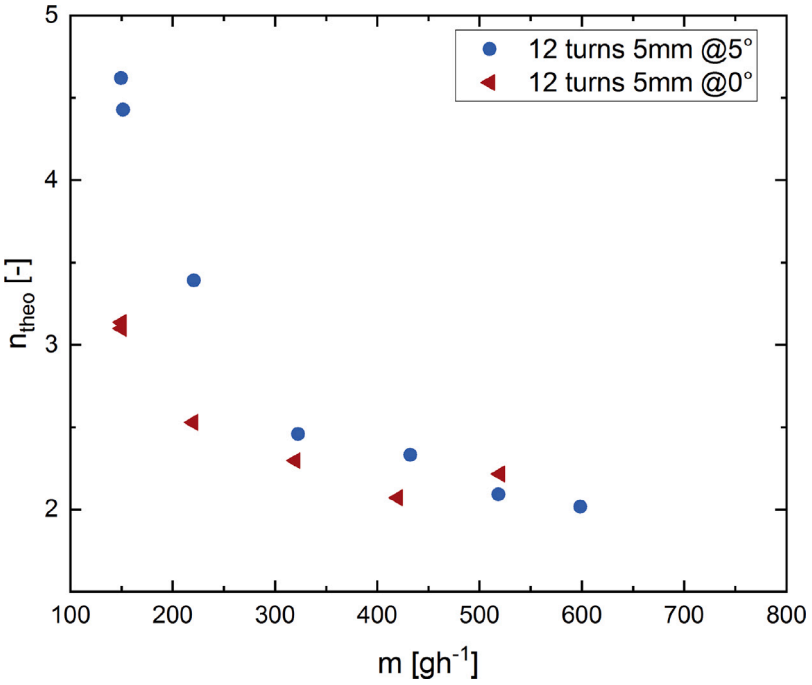

Fig. 13. Separation efficiencies for "HeliDistUnits" PV with $n_{\text{turns}} = 12$ with a channel height h_{channel} of 5 mm for the complete operation range of from 150 g h^{-1} to the flooding point and angular deviation $\Delta\alpha = 5°$ and $\Delta\alpha = 0°$.

experiments. This confirms the significant effect of the mounting angle on the separation efficiency.

4.5. Operating range

The previous section identified the mounting angle as an important noise factor. A close control of this factor ensured the characterization of the maximum operating range of the units. The results are depicted in Fig. 13. The experiments show a strong correlation between the flow rate and the separation efficiency for loads $m_{\text{bottom}} \lesssim 300\,\text{g h}^{-1}$. Only in this operation range the inclination of the units has a major influence on the separation performance. At higher loads, the reached separation efficiency is quite stable reaching around 2 theoretical plates for 12 turns regardless the inclination and load. Making the units especially in 45°-orientation interesting for applications where a constant *HETP* value is needed, like fluctuating feeds or scale-up investigations. For small loads the best *HETP* values are reached with down to around 13 mm. In comparison to micro distillation apparatuses described in literature the values are quite promising. The distillation column of Mardani et al. [16] reached maximum loads of around 200 g h^{-1} with 1.4 theoretical plates per 15 cm. The maximum separation they reached were at 80 g h^{-1} with 4.6 theoretical plates. The apparatus described by Ziogas et al. [8] did not allow to measure the actual loads, however the experiments were conducted with a feed flow rate of 0.5 g per minute reaching 11 mm. Also the values of Podbielniak [9] are reached, however with a wider diameter of the column of 25 mm instead of 13 mm.

5. Conclusion

This work presents a novel additive manufactured modular helical distillation unit. The design is driven by the design guidelines of the PBF-LB\M process to reduce the manufacturing time. First, by testing units with different channel heights, the minimum feasible channel height was determined to $h_{\text{channel}} = 5$ mm. By varying then the number of turns, we could show that the helical channel is decisive for the separation efficiency and no significant inlet/outlet effects exists. However, at low loads an angular dependency was identified allowing to increase the separation efficiency with a tilt of the units of $\Delta\alpha \approx 5°$ by around 50% compared to $\Delta\alpha = 0°$. Also, this relative increase was independent of the number of turns. Cold flow measurements in transparent units revealed that asymmetric channel shape with acute and obtuse corners could be responsible for this effect.

Depending on the channel height, mounting angle and load $HETP_{\text{Helix}}$ values down to 13 mm could be reached. Moreover, it was shown, that the units could be operated at loads up to 500 g h^{-1} to 600 g h^{-1} showing the practical relevance. Also the coupling of different HeliDist units was successfully tested and allows thereby to increase the separation efficiency.

All in all, these first results make the concept look very promising for modular small-scale distillation plants. The next steps are the development of different internals to further increase the separation efficiency and throughput.

6. Nomenclature

The used nomenclature is explained in Table 3.

Table 3
Used nomenclature.

Symbol	Unit	Meaning
α	°	Angle
h_{channel}	m	Height of the helical channel
h	J kg^{-1}	Specific enthalpy
$HETP$	m	Height equivalent to one theoretical plate
m	kg	Mass
$\dot{m}_{\text{bottom}}$	kg h^{-1}	Mass flow of the evaporator
$\dot{m}_{\text{top}}$	kg h^{-1}	Mass flow of the condenser
n_{theo}	–	Number of theoretical plates
n_{turns}	–	Number of turns
ΔQ	W	Heat loss

CRediT authorship contribution statement

Fabian Grinschek: Writing – original draft, Visualization, Validation, Methodology, Investigation, Data curation, Conceptualization. **Jannik Betz:** Writing – review & editing, Investigation. **Chen-Mei Chiu:** Writing – review & editing, Investigation. **Sören Dübal:** Writing – review & editing, Investigation. **Christoph Klahn:** Writing – review & editing, Supervision, Project administration, Funding acquisition. **Roland Dittmeyer:** Writing – review & editing, Supervision, Resources, Project administration, Funding acquisition.

Declaration of competing interest

The authors declare that they have no known competing financial interests or personal relationships that could have appeared to influence the work reported in this paper.

Acknowledgments

The authors would like to thank Manuel Hofheinz und Fabian Rupp IMVT (KIT) for machining the HeliDist units and assistance with the PBF-LB/M machine.

Data availability

Data will be made available on request.

References

[1] H. Kirsch, L. Brübach, M. Loewert, M. Riedinger, A. Gräfenhahn, T. Böltken, M. Klumpp, P. Pfeifer, R. Dittmeyer, CO_2–neutrale Fischer–Tropsch–Kraftstoffe aus dezentralen modularen Anlagen: Status und Perspektiven, Chem. Ing. Tech. 92 (1–2) (2020) 91–99, http://dx.doi.org/10.1002/cite.201900120.

[2] A.T. Sundberg, P. Uusi-Kyyny, V. Alopaeus, Microscale distillation, Russ. J. Gen. Chem. 82 (12) (2012) 2079–2087, http://dx.doi.org/10.1134/S1070363212120286.

[3] E.Y. Kenig, Y. Su, A. Lautenschleger, P. Chasanis, M. Grünewald, Micro-separation of fluid systems: A state-of-the-art review, Sep. Purif. Technol. 120 (2013) 245–264, http://dx.doi.org/10.1016/j.seppur.2013.09.028.

[4] B.C. Kim, H.H. Chun, Y.H. Kim, Energy-efficient diabatic distillation using a horizontal distillation column, Ind. Eng. Chem. Res. 52 (42) (2013) 14927–14935, http://dx.doi.org/10.1021/ie4013997.

[5] D.R. Seok, S.-T. Hwang, Zero-gravity distillation utilizing the heat pipe principle(micro-distillation), AIChE J. 31 (12) (1985) 2059–2065, http://dx.doi.org/10.1002/aic.690311215.

[6] A. Sundberg, P. Uusi-Kyyny, V. Alopaeus, Novel micro-distillation column for process development, Chem. Eng. Res. Des. 87 (5) (2009) 705–710, http://dx.doi.org/10.1016/j.cherd.2008.09.011.

[7] A. Tonkovich, K. Jarosch, R. Arora, L. Silva, S. Perry, J. Mcdaniel, F. Daly, B. Litt, Methanol production FPSO plant concept using multiple microchannel unit operations, Chem. Eng. J. 135 (2008) S2–S8, http://dx.doi.org/10.1016/j.cej.2007.07.014.

[8] A. Ziogas, V. Cominos, G. Kolb, H.-J. Kost, B. Werner, V. Hessel, Development of a microrectification apparatus for analytical and preparative applications, Chem. Eng. Technol. 35 (1) (2012) 58–71, http://dx.doi.org/10.1002/ceat.201100505.

[9] W. Podbielniak, Apparatus and methods for precise fractional-distillation analysis: New design of adiabatic fractioning column and precision-spaced wire packing for temperature range- 190* to 300* C, Ind. Eng. Chem. Anal. Ed. 13 (9) (1941) 639–645, http://dx.doi.org/10.1021/i560097a020.

[10] H.S. Lecky, R.H. Ewell, Spiral screen packing for efficient laboratory fractionating columns, Ind. Eng. Chem. Anal. Ed. 12 (9) (1940) 544–547, http://dx.doi.org/10.1021/ac50149a023.

[11] E. Krell, Handbook of Laboratory Distillation, 3rd completely rev. 2nd ed., Techniques and instrumentation in analytical chemistry, Vol. 2, Elsevier Scientific Pub. Co, 1982.

[12] F.B. Shorland, A simple helical packing for laboratory fractionating columns, J. Appl. Chem. 2 (8) (1952) 438–440, http://dx.doi.org/10.1002/jctb.5010020803.

[13] F.W. Mitchell, J.M. O'Gorman, Helical packing for small laboratory distilling columns, Anal. Chem. 20 (4) (1948) 315–316, http://dx.doi.org/10.1021/ac60016a012.

[14] J. Bower Jr., L. Cooke, Efficient low-holdup laboratory column, Ind. Eng. Chem. Anal. Ed. 15 (4) (1943) 290–293, http://dx.doi.org/10.1021/i560116a028.

[15] L. Bittorf, N. Böttger, D. Neumann, A. Winter, N. Kockmann, Characterization of an automated spinning–band column as a module for laboratory distillation, Chem. Eng. Technol. 44 (9) (2021) 1660–1667, http://dx.doi.org/10.1002/ceat.202000602.

[16] S. Mardani, L.S. Ojala, P. Uusi-Kyyny, V. Alopaeus, Development of a unique modular distillation column using 3D printing, Chem. Eng. Process.: Process Intensif. 109 (2016) 136–148, http://dx.doi.org/10.1016/j.cep.2016.09.001.

[17] J. Neukäufer, N. Sarajlic, H. Klein, S. Rehfeldt, H. Hallmann, C. Knösche, T. Grützner, Flexible distillation test rig on a laboratory scale for characterization of additively manufactured packings, AIChE J. 67 (11) (2021) e17381, http://dx.doi.org/10.1002/aic.17381.

[18] B. Sun, T. Bhatelia, R.P. Utikar, G.M. Evans, V.K. Pareek, Hydrodynamics of a novel 3D printed structured packing–SpiroPak, Chem. Eng. Process.: Process Intensif. 167 (2021) 108533, http://dx.doi.org/10.1016/j.cep.2021.108533.

[19] H. Cong, Z. Zhao, X. Li, H. Li, X. Gao, Liquid-bridge flow in the channel of helical string and its application to gas–liquid contacting process, AIChE J. 64 (9) (2018) 3360–3368, http://dx.doi.org/10.1002/aic.16176.

[20] J. Wang, H. Li, X. Li, H. Cong, X. Gao, An intensification of mass transfer process for gas-liquid counter-current flow in a novel microchannel with limited path for CO2 capture, Process Saf. Environ. Prot. 149 (2021) 905–914, http://dx.doi.org/10.1016/j.psep.2021.03.046.

[21] ASTM International and ISO, ISO/ASTM 52900:2022: Standard terminology for additive manufacturing – general principles – terminology, 2022, ISO/ASTM 52900:2022.

[22] B. Leutenecker-Twelsiek, C. Klahn, M. Meboldt, Considering part orientation in design for additive manufacturing, Procedia CIRP 50 (2016) 408–413, http://dx.doi.org/10.1016/j.procir.2016.05.016.

[23] O. Diegel, A. Nordin, D. Motte, A Practical Guide to Design for Additive Manufacturing, Springer Singapore, Singapore, 2019, http://dx.doi.org/10.1007/978-981-13-8281-9.

[24] F. Grinschek, S. Dübal, C. Klahn, R. Dittmeyer, Einfluss des additiven fertigungsverfahrens auf die gestalt einer mikrorektifikationsapparatur, Chem. Ing. Tech. (2022) http://dx.doi.org/10.1002/cite.202200011.

[25] L.E. Wiesegger, R.P. Knauss, T. Winkler, S. Maikowske, J.J. Brandner, R.J. Marr, Transport phenomena in novel microstructures for use in thermal separation processes, in: Proceedings of the 7th International Conference on Nanochannels, Microchannels and Minichannels - 2009, ASME, New York, 2009, pp. 731–738, http://dx.doi.org/10.1115/ICNMM2009-82098.

[26] M. Khoshvaght-Aliabadi, A. Feizabadi, Compound heat transfer enhancement of helical channel with corrugated wall structure, Int. J. Heat Mass Transfer 146 (2020) 118858, http://dx.doi.org/10.1016/j.ijheatmasstransfer.2019.118858.

[27] F. Grinschek, A. Charles, A. Elkaseer, C. Klahn, S.G. Scholz, R. Dittmeyer, Gas-tight means zero defects - design considerations for thin-walled fluidic devices with overhangs by laser powder bed fusion, Mater. Des. 223 (2022) 111174, http://dx.doi.org/10.1016/j.matdes.2022.111174.

[28] A.T. Sundberg, P. Uusi-Kyyny, K. Jakobsson, V. Alopaeus, Control of reflux and reboil flow rates for milli and micro distillation, Chem. Eng. Res. Des. 91 (5) (2013) 753–760, http://dx.doi.org/10.1016/j.cherd.2012.08.009.

[29] VDI Heat Atlas, SpringerLink Bücher, Springer Berlin Heidelberg, 2010, http://dx.doi.org/10.1007/978-3-540-77877-6.

[30] F. Grinschek, D. Xie, M. Klumpp, M. Kraut, E. Hansjosten, R. Dittmeyer, Regular microstructured elements for intensification of gas–liquid contacting made by selective laser melting, Ind. Eng. Chem. Res. (2019) http://dx.doi.org/10.1021/acs.iecr.9b04548.